ACS Energy LETTERS

http://pubs.acs.org/journal/aelccp

REVIEW

Controlling Dendrite Growth in Solid-State Electrolytes

He Liu, Xin-Bing Cheng, Jia-Qi Huang,* Hong Yuan, Yang Lu, Chong Yan, Gao-Long Zhu, Rui Xu, Chen-Zi Zhao, Li-Peng Hou, Chuanxin He, Stefan Kaskel, and Qiang Zhang*

Cite This: *ACS Energy Lett.* 2020, 5, 833−843

ABSTRACT: Solid-state electrolytes (SSEs) are widely considered as an "enabler" to inhibit dendrite growth of lithium-metal anodes for high-energy and highly safe next-generation batteries. However, recent studies demonstrated that lithium dendrites form in working SSEs. Theoretically, dendrite inhibition can be achieved in perfect SSEs without any defects, while dendrite growth is extensively observed in practical SSEs with poor interface stability, large grain boundaries, voids, and partial electronic conductivity. In this Review, dendrite growth behaviors in SSEs, including polymer and inorganic electrolytes, are comprehensively summarized. The observed dendrite morphology in these SSEs, possible formation mechanisms, and some solutions are analyzed. Clear perspectives and some suggestions are also presented for the further development of SSEs in lithium-metal batteries. This Review intends to shed fresh light on the understanding of dendrite growth in SSEs and the rational design of the architecture and materials for SSEs matching the lithium-metal anode.

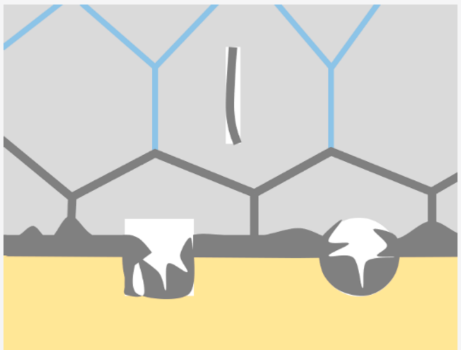

Lithium-ion batteries (LIBs) have revolutionized portable electronic devices and electric vehicles. Next-generation intelligent electronic devices and long-range electric vehicles, however, call for advanced battery systems with higher energy density and safety as well as a longer lifespan. Compared to the graphite anode in commercial LIBs, lithium (Li) metal anode, as the "holy grail" electrode, exhibits an ultrahigh theoretical specific capacity (3860 mAh g^{-1}) and the lowest electrochemical potential (−3.04 V vs the standard hydrogen electrode, graphite anode: 372 mAh g^{-1} and 0.1 V).[1,2] Therefore, a higher energy density can be achieved by the multiplication of capacity and voltage when the Li-metal anode is adopted into a practical battery. However, Li-metal batteries (LMBs) have been long forsaken for use in practical devices because of uncontrollable dendrite growth during repeated cycles, leading to reduced Coulombic efficiency, rapid capacity decay, poor lifespan, and severe safety hazards.[3]

The advances in electrode and electrolyte innovations facilitated by nanoscience and nanotechnology currently offer emerging opportunities to protect the Li-metal anode, such as composite Li electrode, artificial interfacial film, highly concentrated electrolyte (including local high-concentration electrolyte), solid-state electrolyte (SSE), membrane coating, etc.[4,5] Among them, a solid-state electrolyte with a high shear modulus is considered as an effective "enabler" to inhibit dendrite growth.[6−9] In materials science, shear modulus, as one of several quantities for measuring the stiffness of materials, is defined as the ratio of shear stress to the shear strain. Additionally, the features of nonflammability, nonleakage, and high-oxidation voltage as well as low reduction voltage render SSE a promising choice to boost the high-energy-density and safety performance of cells.[10−14] Therefore, SSE is strongly believed to be the ultimate remedy to solve the dendrite growth issues for the development of high-energy-density and highly safe LMBs (Figure 1a).

However, things did not work out the way researchers predicted. The shear modulus criterion proposed by Monroe and Newman is intended only for polymer electrolytes and SSE systems without any inhomogeneities or defects. Dendrites are extensively observed in the SSE systems at the interface or along grain boundaries (GBs), voids, and other soft parts of SSEs (Figure 1b), even at a smaller current and capacity relative to the nonaqueous liquid electrolytes.[15−17] The critical current density, at which the short-circuit occurs by dendrite piercing, is 0.05−0.9 mA cm^{-2} for $Li_7La_3Zr_2O_{12}$ (LLZO) and 0.4−1.0 mA cm^{-2} for $Li_2S{-}P_2S_5$, whereas it reaches 3−10 mA cm^{-2} for

Received: December 7, 2019
Accepted: February 7, 2020
Published: February 7, 2020

https://dx.doi.org/10.1021/acsenergylett.9b02660
ACS Energy Lett. 2020, 5, 833−843

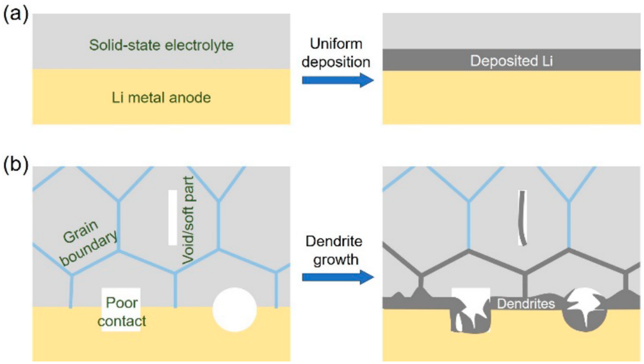

Figure 1. (a) Perfect SSEs without any defects are predicted to inhibit dendrite growth. (b) Inhomogeneous dendritic deposition is observed in practical SSEs.

nonaqueous electrolytes at room temperature.[15] Seemingly, if the testing current density is larger than the critical current density of the SSE, short circuit induced by dendrite growth occurs more easily in SSE systems with inhomogeneities and defects compared to their liquid counterparts, contradicting the prevailing view that dendrites can be inhibited by SSEs with Li-ion transference number approaching 1.0 and shear modulus twice greater than that of Li metal (Figure 2a).[18−21] The detailed mechanism for dendrite formation in SSEs is not fully understood yet.[22] Nevertheless, it is clear that there are distinct mechanism differences for dendrite growth between SSEs and liquid electrolytes.[23,24] Hypotheses are proposed to illustrate the counterintuitive dendrite growth in SSEs, such as small packing density, low ionic conductivity at the GBs, tiny electronic conductivity of bulk electrolytes, random surface and bulk defects formed during SSE preparation, soft parts in the composite SSEs, and poor solid−solid interfacial contact between SSEs and Li metal.[25] The observation of Li-metal penetration through SSEs indicates that a huge gap exists in revealing the relations between structural/chemical/mechanical evolution of SSE interfaces and the electrochemistry of the Li-metal anode.[26,27] Deeply understanding the dendrite growth behaviors in SSEs is critically significant to realize a dendrite-free LMB with SSEs.[28,29]

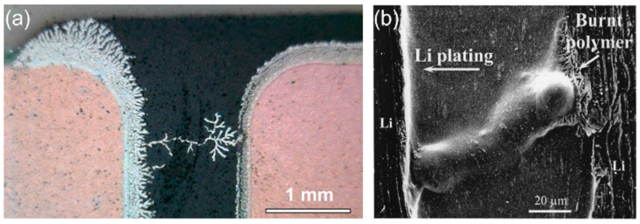

Figure 2. (a) Optical micrograph showing Li dendrites growing along lithium phosphorus oxynitride (LiPON) interface between two Cu current collectors. (Reprinted from ref 19. Copyright 2019 American Chemical Society.) (b) Scanning electron microscopy (SEM) image of a dendrite, just after it has crossed the polymer electrolyte. (Reprinted with permission from ref 37. Copyright 2002 Electrochemical Society.)

In this Review, we summarize the dendrite growth behaviors in the polymer and inorganic SSEs. The observed dendrite growth in these SSEs, the possible mechanisms, and some solutions to suppress dendrite growth are analyzed. The clear perspectives and some suggested directions are also provided for the further development of SSEs in LMBs.

> Seemingly, short circuit induced by Li dendrites is more easily formed in SSE systems compared to their liquid counterparts, contradicting the prevailing view of dendrites that can be inhibited by SSEs with Li-ion transference number approaching 1.0 and shear modulus twice greater than that of Li metal.

Polymer Electrolytes. Polymer electrolytes possess intermediate features between inorganic and nonaqueous electrolytes.[30] For instance, polymer electrolytes exhibit a high mechanical modulus relative to nonaqueous electrolytes and a superior flexibility compared with fragile inorganic electrolytes. These features render polymer electrolytes as potential candidates for practical applications in electric products.[31,32] The demonstration of polymer electrolytes has been well manifested by an electric vehicle, Autolibs, in which the power source is provided by an LMB with a polymeric blend electrolyte composed of poly(ethylene oxide) (PEO)/lithium bis(trifluoromethanesulfonyl)imide (LiTFSI).[18] The polymer electrolyte in this product has to work at a temperature of 40−70 °C to render a high ionic conductivity and uniform Li deposition−dissolution morphology.

Polymer electrolytes are actually unable to completely inhibit the dendrite growth because of their relatively low modulus.[20] For instance, the elastic modulus of a PEO-based electrolyte is approximately 2−3 orders of magnitude less than that of metallic Li.[33] Besides, most polymer electrolytes need to be operated at elevated temperatures to enhance their low room-temperature ionic conductivity. This further reduces their elastic stiffness and increases the tendency of dendrite piercing through SSEs.[34]

Li dendrite growth from metallic Li anode can easily penetrate the soft polymer electrolytes because of their relatively low modulus, leading to cell short circuit and battery failure.[35] Even at a current density as low as 50 μA cm^{-2}, short-circuiting behavior occurs in the PEO/LiTFSI electrolyte after 38 h of polarizing.[36] Dollé and co-workers *in situ* observed Li polymer batteries by scanning electron microscopy. A Li morphology evolution from mossy to dendritic deposition with the increasing current density was confirmed. The dendrites grew outside the polymer and pushed away the Li and the polymer, giving rise to a complete delamination between the electrode and the polymer electrolyte at specific spots, consequently deteriorating the cell performance (Figure 2b).[37]

Local surface inhomogeneities in SSEs play a critical role in the dendric Li plating in Li/polymer batteries.[36,38] The impurity particles prelocated at the Li/SSE interface cause the irregular Li deposition (Figure 3).[39] The impurities are rich in oxygen and electronically insulating, preventing the direct reduction of Li metal on top of them. Instead, Li nucleation and plating are localized at the corner of the impurities because of the increasing local conductivity (Figure 3a). On the other hand, the inhomogeneous Li deposition leads to the generation of voids on the top of the impurities (Figure 3b). The Li/electrolyte interface near the impurities moves upward as the cycling continues, leaving behind the impurity particles at its original

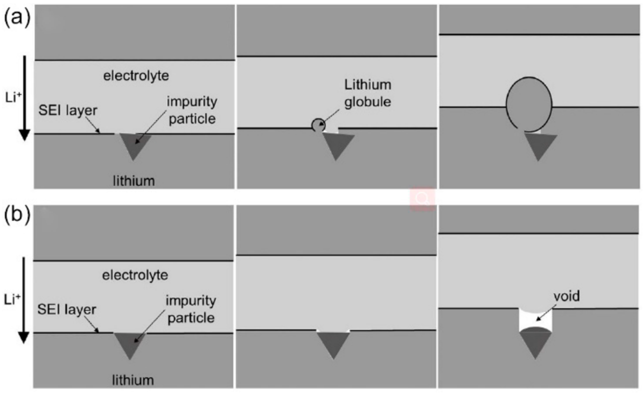

Figure 3. Schematic illustrating the mechanism for (a) Li nucleation and growth at the edge of the impurity particle in a block copolymer electrolyte and (b) the generation of voids on the top of impurities. (Reprinted with permission from ref 39. Copyright 2015 Electrochemical Society.)

location. The degradation of polymer electrolytes caused by the side reactions on top of these impurities separates electrolytes from impurity surface, therefore forming a void between them. The generated voids near the Li/electrolyte interface will in turn aggravate the growth of Li dendrites as discussed later.

Zaghib and co-workers conducted the morphological and chemical analyses of the dendrites in all-solid Li-metal batteries with polyether-based polymer electrolytes and LiTFSI salts.[40] Two morphologies of mossy (Figure 4a) and hollow needles (Figure 4b, c) were observed. Notably, the dendrites herein are composed of Li_xC_y, Li_2O, and $Li_xC_yO_z$ rather than pure metallic Li as universally recognized. The carbide nature of the dendrites presents greater hardness than that of pure Li, thus showing the ability to perforate through the polymer electrolyte. However, this phenomenon is less observed in other literature. These products may be highly system-dependent and do not necessarily represent the general composition of all Li dendrites in SSEs. The mechanism for the formation of hollow needles was also proposed: consumption of Li_xC_y in the initially formed dendrites by oxygen and carbon artifacts and CO_2 degassing of the polymer during cycling.

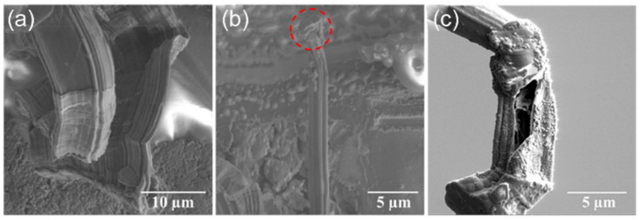

Figure 4. Dendrite growth in a Li-metal battery with polyether-based polymer electrolytes. (Reprinted from ref 40. Copyright 2018 American Chemcial Society.) Dendrites observed *in situ* with (a) mossy and (b and c) hollow needle morphology.

> Li dendrite growth from the metallic Li anode can easily penetrate soft polymer electrolytes because of their relatively low modulus, leading to cell short circuit and battery failure.

Theoretical models have also been presented to evaluate the susceptibility of Li infiltration through polymer SSEs. A kinetic model was proposed incorporating the effects of surface tension and stresses at the interface to derive general criteria for stable Li deposition at solid−solid interfaces.[41] Two separate stable deposition regions in the stability diagram are depicted with different stability mechanisms: pressure-driven in SSEs with a high molar volume ratio and density-driven stability in SSEs with a low molar volume ratio. SSEs with a combination of high (low) molar volume and high (low) shear modulus are required for stable electrodeposition. However, polymer electrolytes generally have a high molar volume ratio but lower shear modulus than the critical value, leading to unstable Li deposition. As a result, material re-engineering at the working interfaces is strongly desired for stable Li deposition.

The propensity of dendrite growth during electrodeposition in polymer-based batteries is strongly related to the applied current density.[42] A cation concentration gradient will be generated in the vicinity of Li anode surfaces at high current densities because of poor Li-ion mobility, leading to the formation of dendric Li deposition. It is critically important to understand the competition between the dendrite growth induced by concentration/potential gradient and suppression rendered by mechanical stress. A phase map was constructed by Barai et al. to clearly depict the stable deposition regime by including the shear modulus of the polymer and the applied current density (Figure 5a).[43] The tendency of dendritic deposition is determined by the actual current density, while high shear modulus of electrolytes results in operating the cell at a higher current without the rise of growing dendrites. The roles of the increased elastic modulus are summarized as follows: (i) Higher compressive stress results in decreased exchange current density in the tips relative to that in the valley. (ii) If the electrolyte has a high shear modulus ($G_{Electrolyte} > 10^{-3}G_{Lithium}$), the height of the dendritic tips can be largely reduced because of the plastic deformation of metallic Li. Besides, the yield strengths of the polymer electrolyte and metallic Li anode severely affect dendrite propagation as well. The yield strength is defined as the stress at which a predetermined amount of permanent deformation occurs. The dendritic tips can be effectively stabilized by enhancing the electrolyte's yield strength, even when the polymer holds an elastic modulus 2 orders of magnitude less than that of metallic Li.

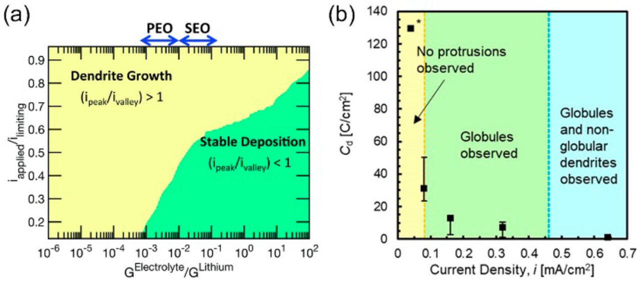

Figure 5. (a) Phase map depicting the stable Li deposition regime including the applied current and the shear modulus of polymer electrolyte. (Reprinted with permission from ref 43. Copyright 2017 Royal Society of Chemistry.) (b) Feature of observed Li protrusions with respect to the current density (i). (Reprinted from ref 44. Copyright 2018 American Chemical Society.)

Maslyn et al. experimentally obtained the current density at which the nonplanar electrodeposition initiates in symmetric

Li−polymer−Li cells using the synchrotron X-ray tomography technique (Figure 5b).[44] The experimentally observed onset current density for nonuniform Li growth is around 20 times lower than the theoretical prediction values reported by Barai et al.[43] This is mainly induced by the presence of impurities in the current Li electrode, which act as the nucleation sites for the inhomogeneous Li deposition. The feature of deposited Li metal depends on the applied current density. Stable Li deposition without any dendrites can be achieved at a low current density below 0.04 mA cm^{-2} (yellow area). Globular protrusions are observed with increased current densities (green area, $0.08 \leq i \leq 0.32$ mA cm^{-2}). Both globular and dendritic deposits are achieved (blue area) at a high current density of 0.64 mA cm^{-2}.

PEO-based polymer is one of the most frequently adopted polymer electrolytes because of its outstanding compatibility with lithium salts, high ionic conductivity, and good electrochemical stability.[45] The addition of inorganic fillers, organic compounds with low molecular weight, and cross-linked electrolytes is developed to improve the Li dendrite growth resistance in the PEO-based polymer electrolyte.[46−48] Some novel polymer electrolytes,[47] interface coating,[49] single-ion solid polymer electrolytes,[50] etc. are also proposed. As the polymer electrolytes especially at a high temperature indicate features similar to those of the nonaqueous electrolyte, some strategies to inhibit dendrite growth in the nonaqueous electrolytes can be implemented in the polymer electrolyte systems.

Inorganic Electrolytes. Inorganic SSEs with a high mechanical strength and compactness are expected to inhibit the Li dendrite penetration through them.[51] Unfortunately, contrary to the general understanding, recent reports have indicated that Li dendrites form easily in inorganic SSEs.[52] Even worse, short circuit initiates at a much lower current or cycling capacity in inorganic SSEs relative to liquid or polymer electrolytes.[53,54] The faster dendrite formation in inorganic SSEs is aggravated by two factors: (i) increased electric driving force due to the larger curvature at dendrite tips because it extends in the limited spaces in the SSEs (such as GBs, defects, voids, etc.)[42] and (ii) less dendrite consumption resulting from the good chemical compatibility and unity transference number of ceramic SSEs.[53]

On the basis of the kinetic model proposed by Ahmad and Viswanathan, the SSEs for stable Li deposition require a combination of high (low) molar volume and high (low) shear modulus.[41] However, typical inorganic SSEs usually have a low molar volume ratio but a higher shear modulus than the critical one, which do not satisfy the criteria and result in unstable Li deposition. GBs in inorganic SSEs are confirmed as the preferential sites for Li dendrite growth considering their softening elastic property and low ionic conductivity compared to the bulk.[55,56] Chiang and colleagues suggested an electrochemomechanical model of Li filled in the preexisted defects to explain the observed Li infiltration through the single crystals.[57] In addition, the partial electronic conductivity of SSEs was considered as the origin for Li nucleation within the SSEs.[15,58,59] Furthermore, the high chemical stability and ionic transference number of inorganic SSEs result in less consumption of Li dendrites during cycling.[53] Therefore, dendrites are gravely aggravated and short circuit the cells at low capacities.[53] These results can present novel insights into SSE designs in high-energy-density and safe battery systems. In the following section, the forming scenarios of dendrite growth induced by poor wettability and unstable electrode/electrolyte interface, grain boundary, void, and electronic conductivity of SSEs are introduced comprehensively.

Dendrite growth in inorganic SSEs can be induced by poor wettability and unstable electrode/electrolyte interface, grain boundaries, voids, and the electronic conductivity of SSEs.

Many ceramic electrolytes, such as LLZO, have surface contaminants, including LiOH, Li_2CO_3, etc.[60,61] The Li-ion diffusion rate in these contaminants is much slower compared to that in ceramic electrolytes. Li ions are forced to diffuse away from areas containing impurities and centralize on the confined contact points at the Li/SSE interface. Therefore, the focusing current at these points leads to inhomogeneous distribution and deposition of Li, which eventually exacerbates the penetration of metallic dendrites into the SSEs (Figure 6a).[55] In this case, cleaning the surface of SSEs[60] and coating with lithiophlic materials on SSE surface[62] are demonstrated to be effective in delaying the onset of Li infiltration even at a higher current density.

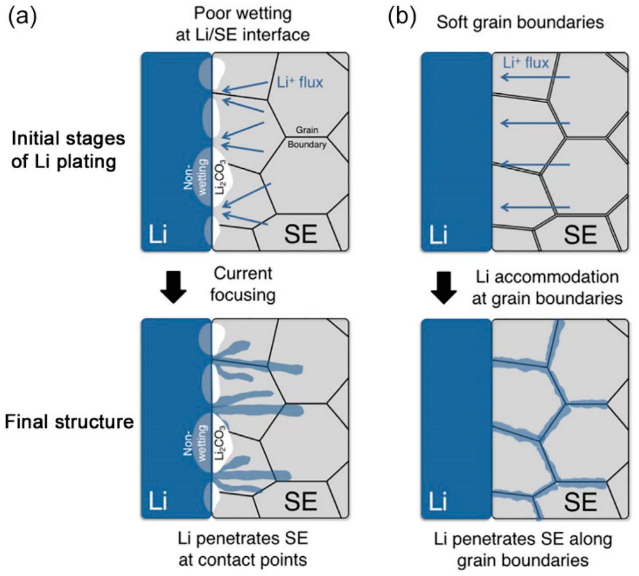

Figure 6. Potential microstructural contributions to dendritic Li deposition in SSEs. (Reprinted from ref 55. Copyright 2018 American Chemical Society.) (a) The presence of surface contaminants leads to the current focusing in SSEs. (b) Li preferentially accumulates in the softer regions close to the electrode/GB junction.

The GB is another site in inorganic SSEs for Li dendrite propagation. Significant softening in elastic properties near the GBs is proposed as the origin for dendrite growth in these sites (Figure 6b).[55] The variations in atomic structure and density in the vicinity of the GB plane lead to the decrease in the elastic modulus in this area.[63] Molecular dynamics simulations reveal that the shear modulus at GBs can be as high as 50% lower than that in the bulk regions. This inhomogeneous elastic property leads to deposited Li atom accumulation in softer regions near electrode/GB junctions during Li plating.[26,64] Consequently, locally stronger electric fields will be generated in the resulting Li protrusions, becoming the “hot spots” for the subsequent Li deposition. Consequently, the counterintuitive observation that soft Li metal penetrates ostensibly stiff inorganic SSEs could be rationalized by the existing GB "soft spots".

Another driving force for Li dendrite growing along the GBs is the gap in the ionic conductivity between bulk and GB regions in SSEs. The bottleneck for achieving a high ionic conductivity in SSEs frequently lies in the significantly lower GB conductivity compared to the bulk (Figure 7a).[56,65−69] Molecular dynamics simulations predict that Li-ion mobility through the GBs is largely reduced, and Li-ion migration activation energy for all GBs is consistently higher relative to the bulk SSEs.[65,68] Ma et al. experimentally unraveled the atomic-scale reason for the low GB conductivity in $(Li_{3x}La_{2/3-x})TiO_3$. A severe structural and chemical deviation is discovered at the GBs consisting of a Ti−O binary phase with a thickness of 2−3 unit cells. Such a structure is not favorable for Li^+ storage and transport, leading to the high GB resistance. This results in Li dendrites preferentially propagating along the GBs (Figure 7b−d).[64,70] Processing SSEs to achieve a high fraction of low energy and compact boundaries can efficiently modify the GB conductivity and regulate dendrite growth behaviors. For example, modifying the SSEs by element doping,[17,71,72] carbon posttreatment,[73] sintering,[74] and hot-pressing,[75] as well as directly modifying the GBs with Li_2CO_3/LiOH[76] and additional Li,[77] can improve the GB conductivity and the critical current density of SSEs.

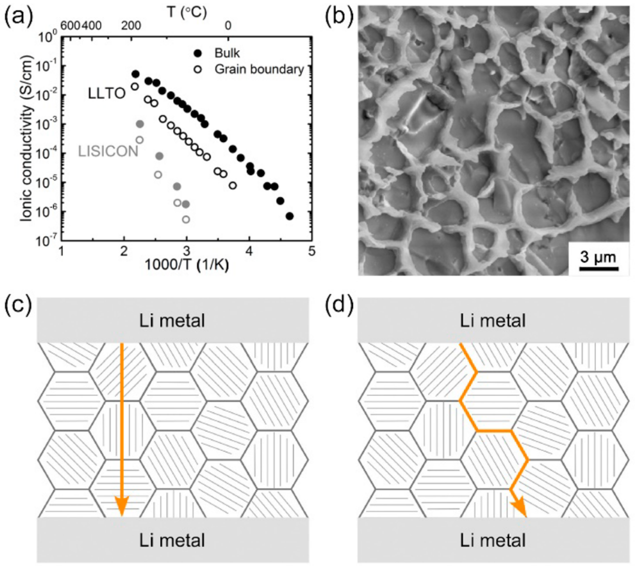

Figure 7. (a) Ionic conductivities at bulk and grain-boundary regions with respect to temperature in $Li_{0.34}La_{0.51}TiO_{2.94}$ (LLTO) and $Li_{2+2x}Zn_{1-x}GeO_4$ (LISICON, $x = 0.55$). (Reprinted from ref 56. Copyright 2016 American Chemical Society.) (b) SEM image showing web-structure Li-metal plating along the GBs in the bulk LLZO.[64] Schematic of Li metal (c) transgranular and (d) intergranular plating in polycrystalline LLZO SSEs. (Reprinted with permission from ref 64. Copyright 2017 Elsevier.)

Preexisting voids and cracks in inorganic SSEs or near the Li/SSE interface are also suspicious spots for the formation of Li dendrites. In an all-solid-state LMB with inorganic SSEs, a crack or void in the SSE near the Li-metal electrode can be easily penetrated by Li deposition because of the electric field amplification, inevitably forming dendrites in these sites.[78,79] Further insertion of Li into the cracks accompanies the generation of pressure in SSEs (Figure 8).[1] The pressure in the cracks increases very rapidly, reaching up to 1 GPa within seconds even at normal charging rates. The high pressure will in turn promote the propagation of cracks and release the pressure in the crack. However, the high pressure will be rebuilt rapidly in the longer crack, resulting in further crack extension. This process repeats until the crack reaches the cathode, finally short-circuiting the battery.[80]

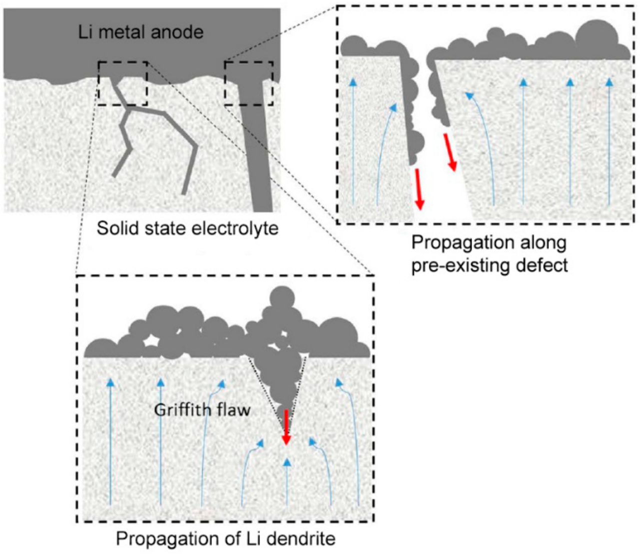

Figure 8. Schematic of Li growth at the preexisting interfacial defects (Griffith flaw: a crack that propagates when the reduction in potential energy that occurs due to crack growth is greater than or equal to the increase in surface energy due to the creation of new free surfaces) in SSEs and propagation of lithium along the preexisted defects. Blue arrows represent the electric field lines, and red arrows show the undesired Li-metal growth into the bulk. (Reprinted with permission from ref 1. Copyright 2017 Electrochemical Society.)

Voids formed in Li metal near the electrolyte/electrode interface during cell operation are also propagation sites for Li dendrites. When Li metal is stripped above the critical current at which Li removal rate exceeds that at which the Li can be replenished, voids form in the Li anode near the interface. In addition, the stripping process first occurs to the Li-metal anode when it matches a Li-free cathode, such as sulfur and oxygen. In this case, voids form on the Li metal close to the interface initially and accumulate in the following cycles.[81] Li plating initiates at the interface where Li metal contacts the SSEs to obtain Li ions and electrons simultaneously and then grows unhindered along the voids. Therefore, Li deposition preferentially occurs at the triple point where Li metal, SSE, and voids meet.[82] Irreversible pulverization of Li metal resulting from extended and interconnected cracks after long cycles further exacerbates the propagation of dendrites.[83] Additionally, voids near the interface deteriorate the interfacial contact between SSE and Li metal and elevate the local plating current density, leading to the formation of dendrites in the pregenerated voids.[82]

It is important to reveal the relation between Li dendrite propagation and microstructure evolution of SSEs. Pylypenko and co-workers *in operando* detected the Li dendrite growth in the voids and the void evolution during repeated cycles in a symmetric Li/β-Li_3PS_4/Li cell by synchrotron-based X-ray tomography (Figure 9).[84] The expansion of voids as the cycling proceeds can be observed throughout the whole cell. This extension in void width resembles crack propagation caused by

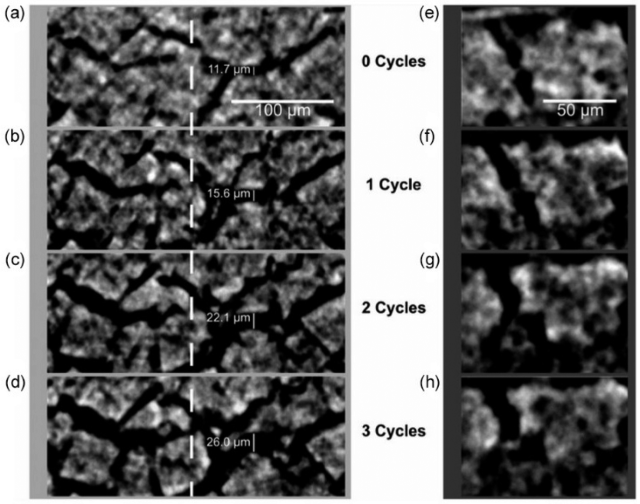

Figure 9. Synchrotron-based X-ray tomography monitoring void expansion and Li evolution in a symmetric cell with β-Li_3PS_4 SSEs cycled at 100 μA cm^{-2} at early stages of cycling. (Reprinted with permission from ref 84. Copyright 2018 Electrochemical Society.)

interactions between Li metal and voids in the β-Li_3PS_4 electrolyte. As a result, the void expansion can be assigned to the dendrite growth into the SSE bulk region. The continued dendrite growth after the void space is occupied will destroy the grains of β-Li_3PS_4, further promoting Li dendrite propagation within the SSE and deteriorating the cell performance. Therefore, SSEs with connected pore regions aggravate dendrite growth and short circuit the cell at a lower critical current density relative to the samples with less interconnected pores.[85] Densifying SSEs and homogeneous Li metal/SSE interfaces with less voids and cracks are necessary to prevent dendrite growth in inorganic SSE systems.[86] Element doping,[87,88] interstitial filler,[89] and synthesis condition optimization[75,85,90] are effective strategies to densify SSEs (relative density > 99%) and mitigate the dendrite growth.

Electronic conductivity is also a vital factor to affect the Li dendrite growth in SSEs.[91,92] The electronic conductivity of SSEs may give rise to Li-metal growth directly within the bulk of SSEs, especially within the intrinsic GB/pores of the SSE, rather than uniaxial growth from the Li/SSE interface to SSE.[89] Qi and colleagues investigated the Li dendrite formation and growth inside SSEs through a multiscale modeling by integrating density functional theory calculations and phase field simulations.[59,93] The lower band gap at surfaces (pores and cracks) compared to that in the bulk facilitates electron transport from Li metal to the surface. The trapped excess electrons on the surfaces allow isolated Li nucleation and accelerated Li dendrite growth.

Han et al. compared the formation behaviors of Li dendrites in three representative SSEs (LLZO, Li_3PS_4, and LiPON) and found that ionic conductivity is also a possible reason for dendrite growth in the SSE.[15] By comparing the relative density, shear modulus, interfacial resistance, and ionic conductivity of LLZO and LiPON, they predicted that LLZO should exhibit dendrite inhibition ability similar to that of LiPON. In fact, dendrites grow severely in LLZO than in LiPON. Therefore, some other parameters determine the tendency of dendrite growth. Instead, the critical current density of SSEs correlates well with their electronic conductivities. The LLZO and $Li_2S-P_2S_5$ present electronic conductivities several orders of magnitude higher relative to that of LiPON, whereas the former two SSEs exhibit much lower critical current densities compared to LiPON. This is because the high electronic conductivity renders it easier for Li^+ to receive electrons and directly generate Li dendrites within the SSEs. Consequently, the high electronic conductivity could potentially be the cause of Li dendrite propagation in these SSEs. Additionally, the homogeneous and pore-free morphology of LiPON also contributes to its dendrite suppression capability.[19] This work provides another direction in regulating Li-metal growth and indicates the need to lower the electronic conductivity of SSEs to alleviate dendrite formation.

Unlike ceramic SSEs (such as LLZO, Li_3OX (X = Cl, Br), $LiBH_4$, etc.), another category of SSEs (including $Li_7P_3S_{11}$ (LPS), $Li_{10}GeP_2S_{12}$ (LGPS), $Li_{1.4}Al_{0.4}Ge_{1.6}(PO_4)_3$ (LAGP), etc.) is not stable against the Li-metal anode.[94−96] (Electro)-chemical reactions occur between the Li-metal anode and these electrolytes, and the formed solid electrolyte interphase (SEI) will definitely transform the interfaces and affect the dendrite growth behaviors in SSEs.[27,97] LAGP is chemically and electrochemically active toward Li.[98] The chemically formed interphase between Li metal and LAGP before electrochemical reactions exhibits a mixed ionic and electronic conductivity with the electronic conductivity dominating.[99] This interface strongly affects the electrical properties, mechanical integrity, and thermal stability of SSEs. Two possible electrochemical reaction pathways occur at this mixed-conducting interphase (Figure 10).[97] In pathway 1, LAGP is electrochemically reduced at the LAGP/interphase boundary by obtaining Li ions with electrons traversing the mixed-conducting interphase. Nonuniform Li deposition is accelerated through pathway 1 because of the decrease in the Li^+ transport distance (d_1 compared to d_2) and thereby lowering the local ion conduction resistance. This shortened ion transport length will be amplified at higher currents because of the overall higher overpotential, resulting in a severely inhomogeneous plating morphology. Li deposition also occurs at the Li/LAGP interface as illustrated in pathway 2 (Figure 10). This reduction pathway will not cause the electrochemical formed interphase. The two pathways are in competition in this system depending on the operating current density.[97] The desired Li/electrolyte interphase needs to combine the features of high ionic conductivities, low electronic conductivities, and high chemical stability to suppress the formation of Li dendrites and realize stable and safe solid-state batteries.

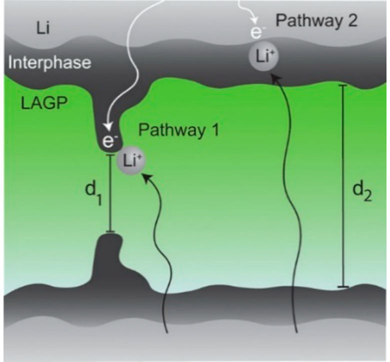

Figure 10. Schematic illustrating possible reaction pathways and nonuniform evolution at Li/LAGP interphase with a mixed-conducting interphase. (Reprinted from ref 97. Copyright 2019 American Chemical Society.)

In short, the growth of Li dendrites in SSEs proceeds in two steps: dendrite nucleation and its subsequent propagation inside SSEs. The nucleation sites can be at the Li/electrolyte interface or inside the bulk SSEs depending on the surface chemistry and electronic conductivity of SSEs as well as the operating current density/capacity.[2] Upon nucleation, Li dendrites tend to expand along the defects inside the SSEs, such as GBs, voids, cracks, etc. The dendrite growth in SSEs follows different paths in different SSE systems and current densities/capacities. Once dendrites grow into a large diameter, they give rise to the concentrated mechanical stress between Li metal and SSEs, crack propagation, and even degradation of SSEs. In addition, some very thin and tiny dendrites grow and short circuit the batteries before they can be detected. In this case, the main driving force should be the enhanced local electrical field caused by the larger curvature at dendrite tips in the limited space of defects in SSEs.

Summary and Outlook. SSEs are receiving great research interest because of their nonflammability, nonleakage features, and high-oxidation voltage as well as low reduction voltage, which are promising for rendering highly safe and high-energy-density batteries. Their high mechanical modulus compared to that of nonaqueous electrolytes has the potential to inhibit the dendrite growth of metallic Li as well. However, when SSEs match Li metal or other intercalation anodes even at moderate conditions, dendrite growth is observed between the interface of SSEs and anode, or inside the SSEs.

Li dendrites form in polymer SSEs because of their relatively low modulus and surface impurities. Applied current density and pressure also affect the propensity for dendrite growth. In inorganic SSEs, dendrite growth can be contributed by the poor wettability and unstable electrode/electrolyte interface, grain boundary, void, and electronic conductivity of SSEs. Theoretically, if SSEs are perfect without any defect, dendrites cannot grow through SSEs, especially the rigid ceramics. However, it is nearly impossible to obtain a perfect electrolyte. To realize the large-scale application of fragile ceramic electrolytes, hybridizing of flexible polymer and rigid ceramic electrolytes is regarded as a promising route to obtain practical SSEs, where hard and soft components contribute in the composite SSEs synergetically.[46] Apparently, dendrite growth easily occurs in the soft part of the composite SSE. Therefore, for future research on SSEs matching Li-metal anode, many more efforts are required to concentrate on the interfacial and bulk features of SSEs. Some suggested directions are presented herein.

(1) Detailed mechanisms of dendrite evolution in SSEs. Fundamental questions on the mechanisms depicting the dynamic processes of Li nucleation, propagation, interface migration, and crack evolution in SSE system still remain open. For example, how do the surface chemistry and interfacial properties of SSEs affect the dynamic processes of Li dendrite growth? What is the influence of electric potential distribution at the dendrite tips and distribution of electronic and ionic transport channels in SSEs on the dendrite growth? These remaining questions require further in-depth investigation.

(2) Facile characterization techniques. Powerful and facile characterization methods to track the detailed and in-depth interfacial evolution information on SSEs are lacking.[100] Because of the solid feature of SSEs, it is very difficult to *in situ*/*operando* characterize the states of working SSEs. Currently, the frequently applied tool to track the dendritic Li deposition in liquid electrolytes is optical and electron microscopy; however, it cannot provide in-depth information on dendrite growth in SSEs.[101] Elaborate neutron measurements,[15,52,102] X-ray microtomography techniques,[27,84,85,103] and time-of-flight secondary-ion mass spectrometry[53] are always adopted to characterize SSEs. The *operando* or *in situ* microscopy and spectroscopy measurement techniques with higher spatial−temporal distribution and multidimensional resolution are required to obtain more detailed information on the working states, including the morphology and chemistry of interfaces in SSEs.[24]

(3) Simulation methods. Interfacial stability between Li-metal anodes and SSEs has been comprehensively investigated by *ab initio* molecular dynamics simulations.[104] Machine-learning techniques have also been proposed to computationally screen SSEs with simultaneous dendrite-suppression capability and high ionic conductivity.[105] Rarely are research works conducted on the dendrite growth near the interface between SSEs and Li-metal electrodes and inside the SSEs. Besides molecular dynamics simulations[65,68] and density functional theory calculations,[59] phase field simulations are also required to collaboratively predict dendrite growth in SSEs.[93]

(4) Polymer/ceramic composite electrolytes. Recent research contributions on dendrite growth are mostly conducted in single-polymer or ceramic systems, while fewer are conducted on the basis of the polymer/ceramic composite SSE, which is a quite promising electrolyte system for future practical applications.[106] Information on structure and component distribution, ionic conduction paths, and Li deposition behavior is required for the design of an advanced composite SSE.

(5) Implantation of dendrite-suppression strategies from the protection of Li-metal anodes. Dendrite growth in the Li-metal electrodes has been probed deeply. If Li deposits uniformly on the anode side regulated by the Li-metal anode itself, short circuit by dendrite permeation will be largely relieved in SSEs. Li-metal host and nonaqueous electrolyte wetting are promising methods to regulate Li deposition behaviors. Combinations of these strategies are helpful to realize dendrite-free deposition behavior in SSE systems.

Li-metal anode working with SSEs will be one of the ultimate solutions for the high-energy-density and highly safe battery systems. Future research efforts in this field need to be intelligently focused to achieve dendrite-free Li deposition at the Li/SSE interface and inside SSEs. Exploiting facile tools to probe the structure and morphology evolution of the interfaces and SSEs at different time and space scales helps reveal the relations between SSE features, evolution of morphology dynamics, and electrochemical performance of the Li-metal anode. We hope that this Review can shed new light on the deep understanding of Li dendrite growth in SSE systems. It will also help in the rational design of the architectures and materials for SSEs matching Li-metal anodes to open a new chapter in energy storage systems.

■ AUTHOR INFORMATION

Corresponding Authors

Jia-Qi Huang − *School of Materials Science & Engineering and Advanced Research Institute for Multidisciplinary Science, Beijing Institute of Technology, Beijing 100081, China;* orcid.org/0000-0001-7394-9186; Email: jqhuang@bit.edu.cn

Qiang Zhang − *Beijing Key Laboratory of Green Chemical Reaction Engineering and Technology, Department of Chemical Engineering, Tsinghua University, Beijing 100084, P.R. China;* orcid.org/0000-0002-3929-1541; Email: zhang-qiang@mails.tsinghua.edu.cn

Authors

He Liu − *School of Materials Science & Engineering and Advanced Research Institute for Multidisciplinary Science, Beijing Institute of Technology, Beijing 100081, China*

Xin-Bing Cheng − *Beijing Key Laboratory of Green Chemical Reaction Engineering and Technology, Department of Chemical Engineering, Tsinghua University, Beijing 100084, P.R. China;* orcid.org/0000-0001-7567-1210

Hong Yuan − *School of Materials Science & Engineering, Beijing Institute of Technology, Beijing 100081, China*

Yang Lu − *Beijing Key Laboratory of Green Chemical Reaction Engineering and Technology, Department of Chemical Engineering, Tsinghua University, Beijing 100084, P.R. China*

Chong Yan − *School of Materials Science & Engineering, Beijing Institute of Technology, Beijing 100081, China;* orcid.org/0000-0001-9521-4981

Gao-Long Zhu − *Beijing Key Laboratory of Green Chemical Reaction Engineering and Technology, Department of Chemical Engineering, Tsinghua University, Beijing 100084, P.R. China; Shenzhen Key Laboratory of Functional Polymer, College of Chemistry and Chemical Engineering, Shenzhen University, Shenzhen 518000, China*

Rui Xu − *School of Materials Science & Engineering, Beijing Institute of Technology, Beijing 100081, China*

Chen-Zi Zhao − *Beijing Key Laboratory of Green Chemical Reaction Engineering and Technology, Department of Chemical Engineering, Tsinghua University, Beijing 100084, P.R. China;* orcid.org/0000-0002-1794-3086

Li-Peng Hou − *Beijing Key Laboratory of Green Chemical Reaction Engineering and Technology, Department of Chemical Engineering, Tsinghua University, Beijing 100084, P.R. China*

Chuanxin He − *Shenzhen Key Laboratory of Functional Polymer, College of Chemistry and Chemical Engineering, Shenzhen University, Shenzhen 518000, China;* orcid.org/0000-0002-2254-360X

Stefan Kaskel − *Department of Inorganic Chemistry, Dresden University of Technology, 01069 Dresden, Germany; Fraunhofer Institute for Material and Beam Technology, 01277 Dresden, Germany;* orcid.org/0000-0003-4572-0303

Complete contact information is available at: https://pubs.acs.org/10.1021/acsenergylett.9b02660

Notes

The authors declare no competing financial interest.

Biographies

He Liu received her Ph.D. degree from Institute of Process Engineering, Chinese Academy of Sciences in 2017. She is currently conducting her postdoctoral research in Jia-Qi Huang's group. Her current research interests mainly focus on the structure design of Li-metal anodes and solid-state electrolytes. http://orcid.org/0000-0003-1853-4732

Xin-Bing Cheng received his B.Eng. (2012) from Tianjin University and Ph.D. (2017) degrees from Tsinghua University, China. He is a research assistant at Tsinghua University. His current research interests mainly focus on energy storage materials and devices. http://orcid.org/0000-0001-7567-1210

Jia-Qi Huang received his B.Eng. (2007) and Ph.D. (2012) degrees from Tsinghua University, China. Now he is a professor at Beijing Institute of Technology. His research interests focus on synthetic approaches and application of nanomaterials for rechargeable batteries, including Li−S batteries, Li-metal anodes, etc. https://orcid.org/0000-0001-7394-9186

Hong Yuan received his Ph.D. degree from Beijing Institute of Technology in 2017. Now he is an associate professor at Advanced Research Institute of Multidisciplinary Science in Beijing Institute of Technology. His research interests are focused on advanced Li−S batteries, Li-ion batteries, and solid-state batteries. http://orcid.org/0000-0001-7565-2204

Yang Lu completed his bachelor's degree at Tianjin University and Ph. D. degree at Shanghai Institute of Ceramics, Chinese Academy of Science. Now he is a postdoctoral researcher in Prof. Qiang Zhang's group in Tsinghua University. His current research focuses on solid-state electrolytes and their interfacial modifications. https://orcid.org/0000-0002-0946-7155

Chong Yan gained his bachelor's and master's degrees from Henan Normal University and is currently a Ph.D. candidate at Beijing Institute of Technology. His current research focuses on the formation of electrode/electrolyte interface and the transport mechanism of Li^+ in the solid electrolyte interphase. https://orcid.org/0000-0001-9521-4981

Gao-Long Zhu obtained his Ph.D. from School of Physics in University of Electronic Science and Technology of China in 2018. He is now a postdoc in Department of Chemical Engineering, Tsinghua University. His main areas of research address energy-storage materials, including solid electrolytes and separators. https://orcid.org/0000-0001-7860-5729

Rui Xu received his B.Eng. in Chemical Engineering from Beijing Institute of Technology in 2017. He subsequently joined Prof. Jia-Qi Huang's group as a Ph.D. student at Beijing Institute of Technology. His research interest is the interface design of stable lithium−metal batteries. https://orcid.org/0000-0001-6439-8706

Chen-Zi Zhao obtained her B.Eng. from School of Materials Science and Engineering in Tsinghua University (2015). She is now a Ph.D. candidate in Department of Chemical Engineering, Tsinghua University. Her main areas of research address energy-storage materials, including solid electrolytes and Li-metal anodes. https://orcid.org/0000-0002-1794-3086

Li-Peng Hou obtained his B.S. degree at Tianjin University in 2018. He is currently a Ph.D. student under the supervision of Prof. Qiang Zhang at the Department of Chemical Engineering, Tsinghua University. His research interests focus on Li-metal batteries, especially the interface in Li−S batteries. https://orcid.org/0000-0002-9147-525X

Chuanxin He is now the Assistant Dean of College of Chemistry and Environmental Engineering, Shenzhen University. His current research interest is the design and synthesis of novel nanostructure materials for fuel cells, water splitting, and electrochemical reduction of carbon dioxide. https://orcid.org/0000-0002-2254-360X

Stefan Kaskel became full professor for Inorganic Chemistry at Technical University Dresden in 2004. Since 2008 he has also worked part time for Fraunhofer IWS, Dresden. His research interests are focused on porous and nanostructured materials for applications in energy storage, catalysis, batteries, and separation technologies. https://orcid.org/0000-0003-4572-0303

Qiang Zhang is a full professor at Tsinghua University. His interests focus on energy materials (Li-metal anodes, Li−S batteries, and electrocatalysis). Currently, he is the associate editor of *Journal of Energy Chemistry* and a member of the advisory board for *Matter*, *Advanced Functional Materials*, *EnergyChem*, *Energy Storage Materials*, and so on. http://orcid.org/0000-0002-3929-1541

ACKNOWLEDGMENTS

This work was supported by National Key Research and Development Program (2016YFA0202500 and 2016YFA0200102), National Natural Science Foundation of China (21676160, 21825501, 21805161, 21808121, and U1801257), and China Postdoctoral Science Foundation (2018M631480 and BX20170012S).

REFERENCES

(1) Kerman, K.; Luntz, A.; Viswanathan, V.; Chiang, Y.-M.; Chen, Z. Review—Practical Challenges Hindering the Development of Solid State Li Ion Batteries. *J. Electrochem. Soc.* **2017**, *164*, A1731−A1744.

(2) Famprikis, T.; Canepa, P.; Dawson, J. A.; Islam, M. S.; Masquelier, C. Fundamentals of Inorganic Solid-State Electrolytes for Batteries. *Nat. Mater.* **2019**, *18*, 1278−1291.

(3) Zhang, X.-Q.; Zhao, C.-Z.; Huang, J.-Q.; Zhang, Q. Recent Advances in Energy Chemical Engineering of Next-Generation Lithium Batteries. *Engineering* **2018**, *4*, 831−847.

(4) Zhao, C.-Z.; Duan, H.; Huang, J.-Q.; Zhang, J.; Zhang, Q.; Guo, Y.-G.; Wan, L.-J. Designing Solid-State Interfaces on Lithium-Metal Anodes: A Review. *Sci. China: Chem.* **2019**, *62*, 1286−1299.

(5) Cheng, X.-B.; Zhang, R.; Zhao, C.-Z.; Zhang, Q. Toward Safe Lithium Metal Anode in Rechargeable Batteries: A Review. *Chem. Rev.* **2017**, *117*, 10403−10473.

(6) Xu, H.; Chien, P.-H.; Shi, J.; Li, Y.; Wu, N.; Liu, Y.; Hu, Y.-Y.; Goodenough, J. B. High-Performance All-Solid-State Batteries Enabled by Salt Bonding to Perovskite in Poly(ethylene oxide). *Proc. Natl. Acad. Sci. U. S. A.* **2019**, *116*, 18815.

(7) Zeng, X.-X.; Yin, Y.-X.; Li, N.-W.; Du, W.-C.; Guo, Y.-G.; Wan, L.-J. Reshaping Lithium Plating/Stripping Behavior via Bifunctional Polymer Electrolyte for Room-Temperature Solid Li Metal Batteries. *J. Am. Chem. Soc.* **2016**, *138*, 15825−15828.

(8) Hou, L.-P.; Yuan, H.; Zhao, C.-Z.; Xu, L.; Zhu, G.-L.; Nan, H.-X.; Cheng, X.-B.; Liu, Q.-B.; He, C.-X.; Huang, J.-Q.; Zhang, Q. Improved Interfacial Electronic Contacts Powering High Sulfur Utilization in All-Solid-State Lithium−Sulfur Batteries. *Energy Storage Mater.* **2020**, *25*, 436−442.

(9) Cheng, X.-B.; Zhao, C.-Z.; Yao, Y.-X.; Liu, H.; Zhang, Q. Recent Advances in Energy Chemistry between Solid-State Electrolyte and Safe Lithium-Metal Anodes. *Chem.* **2019**, *5*, 74−96.

(10) Samson, A. J.; Hofstetter, K.; Bag, S.; Thangadurai, V. A Bird's-Eye View of Li-Stuffed Garnet-Type $Li_7La_3Zr_2O_{12}$ Ceramic electrolytes for Advanced All-Solid-State Li Batteries. *Energy Environ. Sci.* **2019**, *12*, 2957−2975.

(11) Cortes, F. J. Q.; Lewis, J. A.; Tippens, J.; Marchese, T. S.; McDowell, M. T. How Metallic Protection Layers Extend the Lifetime of NASICON-Based Solid-State Lithium Batteries. *J. Electrochem. Soc.* **2020**, *167*, 050502.

(12) Sun, N.; Liu, Q.; Cao, Y.; Lou, S.; Ge, M.; Xiao, X.; Lee, W.-K.; Gao, Y.; Yin, G.; Wang, J.; Sun, X. Anisotropically Electrochemo-Mechanical Evolution in Solid-State Batteries and Interfacial Tailored Strategy. *Angew. Chem., Int. Ed.* **2019**, *58*, 18647−18653.

(13) Zhao, C.-Z.; Chen, P.-Y.; Zhang, R.; Chen, X.; Li, B.-Q.; Zhang, X.-Q.; Cheng, X.-B.; Zhang, Q. An Ion Redistributor for Dendrite-Free Lithium Metal Anodes. *Sci. Adv.* **2018**, *4*, eaat3446.

(14) Sun, Y.-Z.; Huang, J.-Q.; Zhao, C.-Z.; Zhang, Q. A Review of Solid Electrolytes for Safe Lithium-Sulfur Batteries. *Sci. China: Chem.* **2017**, *60*, 1508−1526.

(15) Han, F.; Westover, A. S.; Yue, J.; Fan, X.; Wang, F.; Chi, M.; Leonard, D. N.; Dudney, N. J.; Wang, H.; Wang, C. High Electronic Conductivity as the Origin of Lithium Dendrite Formation within Solid Electrolytes. *Nat. Energy* **2019**, *4*, 187−196.

(16) Li, G.; Monroe, C. W. Dendrite Nucleation in Lithium-Conductive Ceramics. *Phys. Chem. Chem. Phys.* **2019**, *21*, 20354−20359.

(17) Suzuki, Y.; Kami, K.; Watanabe, K.; Watanabe, A.; Saito, N.; Ohnishi, T.; Takada, K.; Sudo, R.; Imanishi, N. Transparent Cubic Garnet-Type Solid Electrolyte of Al_2O_3-Doped $Li_7La_3Zr_2O_{12}$. *Solid State Ionics* **2015**, *278*, 172−176.

(18) Zhang, H.; Li, C.; Piszcz, M.; Coya, E.; Rojo, T.; Rodriguez-Martinez, L. M.; Armand, M.; Zhou, Z. Single Lithium-Ion Conducting Solid Polymer Electrolytes: Advances and Perspectives. *Chem. Soc. Rev.* **2017**, *46*, 797−815.

(19) Westover, A. S.; Dudney, N. J.; Sacci, R. L.; Kalnaus, S. Deposition and Confinement of Li Metal along an Artificial LiPON−LiPON Interface. *ACS Energy Lett.* **2019**, *4*, 651−655.

(20) Monroe, C.; Newman, J. The Impact of Elastic Deformation on Deposition Kinetics at Lithium/Polymer Interfaces. *J. Electrochem. Soc.* **2005**, *152*, A396−A404.

(21) Wood, K. N.; Noked, M.; Dasgupta, N. P. Lithium Metal Anodes: Toward an Improved Understanding of Coupled Morphological, Electrochemical, and Mechanical Behavior. *ACS Energy Lett.* **2017**, *2*, 664−672.

(22) Ma, J.; Chen, B.; Wang, L.; Cui, G. Progress and Prospect on Failure Mechanisms of Solid-State Lithium Batteries. *J. Power Sources* **2018**, *392*, 94−115.

(23) Albertus, P.; Babinec, S.; Litzelman, S.; Newman, A. Status and Challenges in Enabling the Lithium Metal Electrode for High-Energy and Low-Cost Rechargeable Batteries. *Nat. Energy* **2018**, *3*, 16−21.

(24) Krauskopf, T.; Dippel, R.; Hartmann, H.; Peppler, K.; Mogwitz, B.; Richter, F. H.; Zeier, W. G.; Janek, J. Lithium-Metal Growth Kinetics on LLZO Garnet-Type Solid Electrolytes. *Joule* **2019**, *3*, 2030−2049.

(25) Luo, C.; Ji, X.; Chen, J.; Gaskell, K. J.; He, X.; Liang, Y.; Jiang, J.; Wang, C. Solid-State Electrolyte Anchored with a Carboxylated Azo Compound for All-Solid-State Lithium Batteries. *Angew. Chem., Int. Ed.* **2018**, *57*, 8567−8571.

(26) Lewis, J. A.; Tippens, J.; Cortes, F. J. Q.; McDowell, M. T. Chemo-Mechanical Challenges in Solid-State Batteries. *Trends in Chemistry* **2019**, *1*, 845−857.

(27) Tippens, J.; Miers, J. C.; Afshar, A.; Lewis, J. A.; Cortes, F. J. Q.; Qiao, H.; Marchese, T. S.; Di Leo, C. V.; Saldana, C.; McDowell, M. T. Visualizing Chemomechanical Degradation of a Solid-State Battery Electrolyte. *ACS Energy Lett.* **2019**, *4*, 1475−1483.

(28) Liu, M.; Cheng, Z.; Ganapathy, S.; Wang, C.; Haverkate, L. A.; Tułodziecki, M.; Unnikrishnan, S.; Wagemaker, M. Tandem Interface and Bulk Li-Ion Transport in a Hybrid Solid Electrolyte with Microsized Active Filler. *ACS Energy Lett.* **2019**, *4*, 2336−2342.

(29) Yu, J.; Wang, C.; Li, S.; Liu, N.; Zhu, J.; Lu, Z. Li^+-Containing, Continuous Silica Nanofibers for High Li^+ Conductivity in Composite Polymer Electrolyte. *Small* **2019**, *15*, 1902729.

(30) Zhao, C.; Liang, J.; Zhao, Y.; Luo, J.; Sun, Q.; Liu, Y.; Lin, X.; Yang, X.; Huang, H.; Zhang, L.; Zhao, S.; Lu, S.; Sun, X. Engineering a "Nanonet"-Reinforced Polymer Electrolyte for Long-Life $Li−O_2$ Batteries. *J. Mater. Chem. A* **2019**, *7*, 24947−24952.

(31) Wu, H.; Xu, Y.; Ren, X.; Liu, B.; Engelhard, M. H.; Ding, M. S.; El-Khoury, P. Z.; Zhang, L.; Li, Q.; Xu, K.; Wang, C.; Zhang, J.-G.; Xu, W. Polymer-in-"Quasi-Ionic Liquid" Electrolytes for High-Voltage Lithium Metal Batteries. *Adv. Energy Mater.* **2019**, *9*, 1902108.

(32) Wang, C.; Wang, T.; Wang, L.; Hu, Z.; Cui, Z.; Li, J.; Dong, S.; Zhou, X.; Cui, G. Differentiated Lithium Salt Design for Multilayered PEO Electrolyte Enables a High-Voltage Solid-State Lithium Metal Battery. *Adv. Sci.* **2019**, *6*, 1901036.

(33) Harry, K. J.; Higa, K.; Srinivasan, V.; Balsara, N. P. Influence of Electrolyte Modulus on the Local Current Density at a Dendrite Tip on a Lithium Metal Electrode. *J. Electrochem. Soc.* **2016**, *163*, A2216−A2224.

(34) Geng, H. Z.; Rosen, R.; Zheng, B.; Shimoda, H.; Fleming, L.; Liu, J.; Zhou, O. Fabrication and Properties of Composites of Poly(ethylene oxide) and Functionalized Carbon Nanotubes. *Adv. Mater.* **2002**, *14*, 1387−1390.

(35) Rosso, M.; Brissot, C.; Teyssot, A.; Dollé, M.; Sannier, L.; Tarascon, J.-M.; Bouchet, R.; Lascaud, S. Dendrite Short-Circuit and Fuse Effect on Li/Polymer/Li Cells. *Electrochim. Acta* **2006**, *51*, 5334−5340.

(36) Brissot, C.; Rosso, M.; Chazalviel, J. N.; Lascaud, S. Dendritic Growth Mechanisms in Lithium/Polymer Cells. *J. Power Sources* **1999**, *81−82*, 925−929.

(37) Dollé, M.; Sannier, L.; Beaudoin, B.; Trentin, M.; Tarascon, J.-M. Live Scanning Electron Microscope Observations of Dendritic Growth in Lithium/Polymer Cells. *Electrochem. Solid-State Lett.* **2002**, *5*, A286−A289.

(38) Rosso, M.; Gobron, T.; Brissot, C.; Chazalviel, J. N.; Lascaud, S. Onset of Dendritic Growth in Lithium/Polymer Cells. *J. Power Sources* **2001**, *97−98*, 804−806.

(39) Harry, K. J.; Liao, X.; Parkinson, D. Y.; Minor, A. M.; Balsara, N. P. Electrochemical Deposition and Stripping Behavior of Lithium Metal across a Rigid Block Copolymer Electrolyte Membrane. *J. Electrochem. Soc.* **2015**, *162*, A2699−A2706.

(40) Golozar, M.; Hovington, P.; Paolella, A.; Bessette, S.; Lagacé, M.; Bouchard, P.; Demers, H.; Gauvin, R.; Zaghib, K. In Situ Scanning Electron Microscopy Detection of Carbide Nature of Dendrites in Li−Polymer Batteries. *Nano Lett.* **2018**, *18*, 7583−7589.

(41) Ahmad, Z.; Viswanathan, V. Stability of Electrodeposition at Solid-Solid Interfaces and Implications for Metal Anodes. *Phys. Rev. Lett.* **2017**, *119*, 056003.

(42) Raj, R.; Wolfenstine, J. Current Limit Diagrams for Dendrite Formation in Solid-State Electrolytes for Li-Ion Batteries. *J. Power Sources* **2017**, *343*, 119−126.

(43) Barai, P.; Higa, K.; Srinivasan, V. Lithium Dendrite Growth Mechanisms in Polymer Electrolytes and Prevention Strategies. *Phys. Chem. Chem. Phys.* **2017**, *19*, 20493−20505.

(44) Maslyn, J. A.; Loo, W. S.; McEntush, K. D.; Oh, H. J.; Harry, K. J.; Parkinson, D. Y.; Balsara, N. P. Growth of Lithium Dendrites and Globules through a Solid Block Copolymer Electrolyte as a Function of Current Density. *J. Phys. Chem. C* **2018**, *122*, 26797−26804.

(45) Xue, Z.; He, D.; Xie, X. Poly(ethylene oxide)-based electrolytes for lithium-ion batteries. *J. Mater. Chem. A* **2015**, *3*, 19218−19253.

(46) Liu, Y.; Xu, B.; Zhang, W.; Li, L.; Lin, Y.; Nan, C. Composition Modulation and Structure Design of Inorganic-in-Polymer Composite Solid Electrolytes for Advanced Lithium Batteries. *Small* **2019**, *15*, 1902813.

(47) Zhang, X.; Wang, S.; Xue, C.; Xin, C.; Lin, Y.; Shen, Y.; Li, L.; Nan, C.-W. Self-Suppression of Lithium Dendrite in All-Solid-State Lithium Metal Batteries with Poly(vinylidene difluoride)-Based Solid Electrolytes. *Adv. Mater.* **2019**, *31*, 1806082.

(48) Zhao, C.-Z.; Zhang, X.-Q.; Cheng, X.-B.; Zhang, R.; Xu, R.; Chen, P.-Y.; Peng, H.-J.; Huang, J.-Q.; Zhang, Q. An Anion-Immobilized Composite Electrolyte for Dendrite-Free Lithium Metal Anodes. *Proc. Natl. Acad. Sci. U. S. A.* **2017**, *114*, 11069.

(49) Fan, Z.; Ding, B.; Zhang, T.; Lin, Q.; Malgras, V.; Wang, J.; Dou, H.; Zhang, X.; Yamauchi, Y. Solid/Solid Interfacial Architecturing of Solid Polymer Electrolyte−Based All-Solid-State Lithium−Sulfur Batteries by Atomic Layer Deposition. *Small* **2019**, *15*, 1903952.

(50) Cao, C.; Li, Y.; Chen, S.; Peng, C.; Li, Z.; Tang, L.; Feng, Y.; Feng, W. Electrolyte-Solvent-Modified Alternating Copolymer as a Single-Ion Solid Polymer Electrolyte for High-Performance Lithium Metal Batteries. *ACS Appl. Mater. Interfaces* **2019**, *11*, 35683−35692.

(51) Xie, H.; Bao, Y.; Cheng, J.; Wang, C.; Hitz, E. M.; Yang, C.; Liang, Z.; Zhou, Y.; He, S.; Li, T.; Hu, L. Flexible Garnet Solid-State Electrolyte Membranes Enabled by Tile-and-Grout Design. *ACS Energy Lett.* **2019**, *4*, 2668−2674.

(52) Li, Q.; Yi, T.; Wang, X.; Pan, H.; Quan, B.; Liang, T.; Guo, X.; Yu, X.; Wang, H.; Huang, X.; Chen, L.; Li, H. In-Situ Visualization of Lithium Plating in All-Solid-State Lithium-Metal Battery. *Nano Energy* **2019**, *63*, 103895.

(53) Wang, S.; Xu, H.; Li, W.; Dolocan, A.; Manthiram, A. Interfacial Chemistry in Solid-State Batteries: Formation of Interphase and Its Consequences. *J. Am. Chem. Soc.* **2018**, *140*, 250−257.

(54) Han, F.; Yue, J.; Zhu, X.; Wang, C. Suppressing Li Dendrite Formation in Li_2S-P_2S_5 Solid Electrolyte by LiI Incorporation. *Adv. Energy Mater.* **2018**, *8*, 1703644.

(55) Yu, S.; Siegel, D. J. Grain Boundary Softening: A Potential Mechanism for Lithium Metal Penetration through Stiff Solid Electrolytes. *ACS Appl. Mater. Interfaces* **2018**, *10*, 38151−38158.

(56) Bachman, J. C.; Muy, S.; Grimaud, A.; Chang, H.-H.; Pour, N.; Lux, S. F.; Paschos, O.; Maglia, F.; Lupart, S.; Lamp, P.; Giordano, L.; Shao-Horn, Y. Inorganic Solid-State Electrolytes for Lithium Batteries: Mechanisms and Properties Governing Ion Conduction. *Chem. Rev.* **2016**, *116*, 140−162.

(57) Porz, L.; Swamy, T.; Sheldon, B. W.; Rettenwander, D.; Frömling, T.; Thaman, H. L.; Berendts, S.; Uecker, R.; Carter, W. C.; Chiang, Y.-M. Mechanism of Lithium Metal Penetration through Inorganic Solid Electrolytes. *Adv. Energy Mater.* **2017**, *7*, 1701003.

(58) Aguesse, F.; Manalastas, W.; Buannic, L.; Lopez del Amo, J. M.; Singh, G.; Llordés, A.; Kilner, J. Investigating the Dendritic Growth during Full Cell Cycling of Garnet Electrolyte in Direct Contact with Li Metal. *ACS Appl. Mater. Interfaces* **2017**, *9*, 3808−3816.

(59) Tian, H.-K.; Xu, B.; Qi, Y. Computational Study of Lithium Nucleation Tendency in $Li_7La_3Zr_2O_{12}$ (LLZO) and Rational Design of Interlayer Materials to Prevent Lithium Dendrites. *J. Power Sources* **2018**, *392*, 79−86.

(60) Sharafi, A.; Kazyak, E.; Davis, A. L.; Yu, S.; Thompson, T.; Siegel, D. J.; Dasgupta, N. P.; Sakamoto, J. Surface Chemistry Mechanism of Ultra-Low Interfacial Resistance in the Solid-State Electrolyte $Li_7La_3Zr_2O_{12}$. *Chem. Mater.* **2017**, *29*, 7961−7968.

(61) Sharafi, A.; Yu, S.; Naguib, M.; Lee, M.; Ma, C.; Meyer, H. M.; Nanda, J.; Chi, M.; Siegel, D. J.; Sakamoto, J. Impact of Air Exposure and Surface Chemistry on Li−$Li_7La_3Zr_2O_{12}$ Interfacial Resistance. *J. Mater. Chem. A* **2017**, *5*, 13475−13487.

(62) Han, X.; Gong, Y.; Fu, K.; He, X.; Hitz, G. T.; Dai, J.; Pearse, A.; Liu, B.; Wang, H.; Rubloff, G.; Mo, Y.; Thangadurai, V.; Wachsman, E. D.; Hu, L. Negating Interfacial Impedance in Garnet-based Solid-State Li Metal Batteries. *Nat. Mater.* **2017**, *16*, 572.

(63) Adams, J. B.; Wolfer, W. G.; Foiles, S. M. Elastic Properties of Grain Boundaries in Copper and Their Relationship to Bulk Elastic Constants. *Phys. Rev. B: Condens. Matter Mater. Phys.* **1989**, *40*, 9479−9484.

(64) Cheng, E. J.; Sharafi, A.; Sakamoto, J. Intergranular Li Metal Propagation through Polycrystalline $Li_{6.25}Al_{0.25}La_3Zr_2O_{12}$ Ceramic Electrolyte. *Electrochim. Acta* **2017**, *223*, 85−91.

(65) Yu, S.; Siegel, D. J. Grain Boundary Contributions to Li-Ion Transport in the Solid Electrolyte $Li_7La_3Zr_2O_{12}$ (LLZO). *Chem. Mater.* **2017**, *29*, 9639−9647.

(66) Inaguma, Y.; Liquan, C.; Itoh, M.; Nakamura, T.; Uchida, T.; Ikuta, H.; Wakihara, M. High Ionic Conductivity in Lithium Lanthanum Titanate. *Solid State Commun.* **1993**, *86*, 689−693.

(67) Bruce, P. G.; West, A. R. The A-C Conductivity of Polycrystalline LISICON, $Li_{2+2x}Zn_{1-x}$ GeO_4, and a Model for Intergranular Constriction Resistances. *J. Electrochem. Soc.* **1983**, *130*, 662−669.

(68) Dawson, J. A.; Canepa, P.; Famprikis, T.; Masquelier, C.; Islam, M. S. Atomic-Scale Influence of Grain Boundaries on Li-Ion Conduction in Solid Electrolytes for All-Solid-State Batteries. *J. Am. Chem. Soc.* **2018**, *140*, 362−368.

(69) Yu, C.; Ganapathy, S.; van Eck, E. R. H.; van Eijck, L.; de Klerk, N.; Kelder, E. M.; Wagemaker, M. Investigation of Li-Ion Transport in $Li_7P_3S_{11}$ and Solid-State Lithium Batteries. *J. Energy Chem.* **2019**, *38*, 1−7.

(70) Ren, Y.; Shen, Y.; Lin, Y.; Nan, C.-W. Direct Observation of Lithium Dendrites Inside Garnet-Type Lithium-Ion Solid Electrolyte. *Electrochem. Commun.* **2015**, *57*, 27−30.

(71) Pesci, F. M.; Brugge, R. H.; Hekselman, A. K. O.; Cavallaro, A.; Chater, R. J.; Aguadero, A. Elucidating the Role of Dopants in the Critical Current Density for Dendrite Formation in Garnet Electrolytes. *J. Mater. Chem. A* **2018**, *6*, 19817−19827.

(72) Im, C.; Park, D.; Kim, H.; Lee, J. Al-Incorporation into $Li_7La_3Zr_2O_{12}$ Solid Electrolyte Keeping Stabilized Cubic Phase for All-Solid-State Li Batteries. *J. Energy Chem.* **2018**, *27*, 1501−1508.

(73) Li, Y.; Chen, X.; Dolocan, A.; Cui, Z.; Xin, S.; Xue, L.; Xu, H.; Park, K.; Goodenough, J. B. Garnet Electrolyte with an Ultralow

Interfacial Resistance for Li-Metal Batteries. *J. Am. Chem. Soc.* **2018**, *140*, 6448−6455.

(74) Ban, C. W.; Choi, G. M. The Effect of Sintering on the Grain Boundary Conductivity of Lithium Lanthanum Titanates. *Solid State Ionics* **2001**, *140*, 285−292.

(75) David, I. N.; Thompson, T.; Wolfenstine, J.; Allen, J. L.; Sakamoto, J. Microstructure and Li-Ion Conductivity of Hot-Pressed Cubic $Li_7La_3Zr_2O_{12}$. *J. Am. Ceram. Soc.* **2015**, *98*, 1209−1214.

(76) Hongahally Basappa, R.; Ito, T.; Morimura, T.; Bekarevich, R.; Mitsuishi, K.; Yamada, H. Grain Boundary Modification to Suppress Lithium Penetration through Garnet-Type Solid Electrolyte. *J. Power Sources* **2017**, *363*, 145−152.

(77) Chung, H.; Kang, B. Increase in Grain Boundary Ionic Conductivity of $Li_{1.5}Al_{0.5}Ge_{1.5}(PO_4)_3$ by Adding Excess Lithium. *Solid State Ionics* **2014**, *263*, 125−130.

(78) Krauskopf, T.; Mogwitz, B.; Rosenbach, C.; Zeier, W. G.; Janek, J. Diffusion Limitation of Lithium Metal and Li−Mg Alloy Anodes on LLZO Type Solid Electrolytes as a Function of Temperature and Pressure. *Adv. Energy Mater.* **2019**, *9*, 1902568.

(79) Swamy, T.; Park, R.; Sheldon, B. W.; Rettenwander, D.; Porz, L.; Berendts, S.; Uecker, R.; Carter, W. C.; Chiang, Y.-M. Lithium Metal Penetration Induced by Electrodeposition through Solid Electrolytes: Example in Single-Crystal $Li_6La_3ZrTaO_{12}$ Garnet. *J. Electrochem. Soc.* **2018**, *165*, A3648−A3655.

(80) Klinsmann, M.; Hildebrand, F. E.; Ganser, M.; McMeeking, R. M. Dendritic Cracking in Solid Electrolytes Driven by Lithium Insertion. *J. Power Sources* **2019**, *442*, 227226.

(81) Liu, H.; Cheng, X.-B.; Xu, R.; Zhang, X.-Q.; Yan, C.; Huang, J.-Q.; Zhang, Q. Plating/Stripping Behavior of Actual Lithium Metal Anode. *Adv. Energy Mater.* **2019**, *9*, 1902254.

(82) Kasemchainan, J.; Zekoll, S.; Spencer Jolly, D.; Ning, Z.; Hartley, G. O.; Marrow, J.; Bruce, P. G. Critical Stripping Current Leads to Dendrite Formation on Plating in Lithium Anode Solid Electrolyte Cells. *Nat. Mater.* **2019**, *18*, 1105−1111.

(83) Lu, Y.; Huang, X.; Song, Z.; Rui, K.; Wang, Q.; Gu, S.; Yang, J.; Xiu, T.; Badding, M. E.; Wen, Z. Highly Stable Garnet Solid Electrolyte based Li-S Battery with Modified Anodic and Cathodic Interfaces. *Energy Storage Mater.* **2018**, *15*, 282−290.

(84) Seitzman, N.; Guthrey, H.; Sulas, D. B.; Platt, H. A. S.; Al-Jassim, M.; Pylypenko, S. Toward All-Solid-State Lithium Batteries: Three-Dimensional Visualization of Lithium Migration in β-Li_3PS_4 Ceramic Electrolyte. *J. Electrochem. Soc.* **2018**, *165*, A3732−A3737.

(85) Shen, F.; Dixit, M. B.; Xiao, X.; Hatzell, K. B. Effect of Pore Connectivity on Li Dendrite Propagation within LLZO Electrolytes Observed with Synchrotron X-ray Tomography. *ACS Energy Lett.* **2018**, *3*, 1056−1061.

(86) Lu, Y.; Huang, X.; Ruan, Y.; Wang, Q.; Kun, R.; Yang, J.; Wen, Z. An in situ Element Permeation Constructed High Endurance Li−LLZO Interface at High Current Densities. *J. Mater. Chem. A* **2018**, *6*, 18853−18858.

(87) Ren, Y.; Shen, Y.; Lin, Y.; Nan, C.-W. Microstructure Manipulation for Enhancing the Resistance of Garnet-Type Solid Electrolytes to "Short Circuit" by Li Metal Anodes. *ACS Appl. Mater. Interfaces* **2019**, *11*, 5928−5937.

(88) Sudo, R.; Nakata, Y.; Ishiguro, K.; Matsui, M.; Hirano, A.; Takeda, Y.; Yamamoto, O.; Imanishi, N. Interface Behavior Between Garnet-Type Lithium-Conducting Solid Electrolyte and Lithium meMal. *Solid State Ionics* **2014**, *262*, 151−154.

(89) Mo, F.; Ruan, J.; Sun, S.; Lian, Z.; Yang, S.; Yue, X.; Song, Y.; Zhou, Y.-N.; Fang, F.; Sun, G.; Peng, S.; Sun, D. Inside or Outside: Origin of Lithium Dendrite Formation of All Solid-State Electrolytes. *Adv. Energy Mater.* **2019**, *9*, 1902123.

(90) Huang, X.; Lu, Y.; Song, Z.; Rui, K.; Wang, Q.; Xiu, T.; Badding, M. E.; Wen, Z. Manipulating Li_2O Atmosphere for Sintering Dense $Li_7La_3Zr_2O_{12}$ Solid Electrolyte. *Energy Storage Mater.* **2019**, *22*, 207−217.

(91) Song, Y.; Yang, L.; Zhao, W.; Wang, Z.; Zhao, Y.; Wang, Z.; Zhao, Q.; Liu, H.; Pan, F. Revealing the Short-Circuiting Mechanism of Garnet-Based Solid-State Electrolyte. *Adv. Energy Mater.* **2019**, *9*, 1900671.

(92) Cheng, X.-B.; Yan, C.; Zhang, X.-Q.; Liu, H.; Zhang, Q. Electronic and Ionic Channels in Working Interfaces of Lithium Metal Anodes. *ACS Energy Lett.* **2018**, *3*, 1564−1570.

(93) Tian, H.-K.; Liu, Z.; Ji, Y.; Chen, L.-Q.; Qi, Y. Interfacial Electronic Properties Dictate Li Dendrite Growth in Solid Electrolytes. *Chem. Mater.* **2019**, *31*, 7351−7359.

(94) Wenzel, S.; Leichtweiss, T.; Krüger, D.; Sann, J.; Janek, J. Interphase Formation on Lithium Solid Electrolytes—An in situ Approach to Study Interfacial Reactions by Photoelectron Spectroscopy. *Solid State Ionics* **2015**, *278*, 98−105.

(95) Pervez, S. A.; Cambaz, M. A.; Thangadurai, V.; Fichtner, M. Interface in Solid-State Lithium Battery: Challenges, Progress, and Outlook. *ACS Appl. Mater. Interfaces* **2019**, *11*, 22029−22050.

(96) Chen, S.; Xie, D.; Liu, G.; Mwizerwa, J. P.; Zhang, Q.; Zhao, Y.; Xu, X.; Yao, X. Sulfide Solid Electrolytes for All-Solid-State Lithium Batteries: Structure, Conductivity, Stability and Application. *Energy Storage Mater.* **2018**, *14*, 58−74.

(97) Lewis, J. A.; Cortes, F. J. Q.; Boebinger, M. G.; Tippens, J.; Marchese, T. S.; Kondekar, N.; Liu, X.; Chi, M.; McDowell, M. T. Interphase Morphology between a Solid-State Electrolyte and Lithium Controls Cell Failure. *ACS Energy Lett.* **2019**, *4*, 591−599.

(98) Wang, S.; Wang, J.; Liu, J.; Song, H.; Liu, Y.; Wang, P.; He, P.; Xu, J.; Zhou, H. Ultra-Fine Surface Solid-State Electrolytes for Long Cycle Life All-Solid-State Lithium−Air Batteries. *J. Mater. Chem. A* **2018**, *6*, 21248−21254.

(99) Chung, H.; Kang, B. Mechanical and Thermal Failure Induced by Contact between a $Li_{1.5}Al_{0.5}Ge_{1.5}(PO_4)_3$ Solid Electrolyte and Li Metal in an All Solid-State Li Cell. *Chem. Mater.* **2017**, *29*, 8611−8619.

(100) Zhang, C.; Feng, Y.; Han, Z.; Gao, S.; Wang, M.; Wang, P. Electrochemical and Structural Analysis in All-Solid-State Lithium Batteries by Analytical Electron Microscopy: Progress and Perspectives. *Adv. Mater.* **2019**, *31*, 1903747.

(101) Shen, Z.; Zhang, W.; Zhu, G.; Huang, Y.; Feng, Q.; Lu, Y. Design Principles of the Anode−Electrolyte Interface for All Solid-State Lithium Metal Batteries. *Small Methods* **2020**, *4*, 1900592.

(102) Wang, C.; Gong, Y.; Dai, J.; Zhang, L.; Xie, H.; Pastel, G.; Liu, B.; Wachsman, E.; Wang, H.; Hu, L. In Situ Neutron Depth Profiling of Lithium Metal−Garnet Interfaces for Solid State Batteries. *J. Am. Chem. Soc.* **2017**, *139*, 14257−14264.

(103) Harry, K. J.; Hallinan, D. T.; Parkinson, D. Y.; MacDowell, A. A.; Balsara, N. P. Detection of Subsurface Structures Underneath Dendrites Formed on Cycled Lithium Metal Electrodes. *Nat. Mater.* **2014**, *13*, 69−73.

(104) Nolan, A. M.; Zhu, Y.; He, X.; Bai, Q.; Mo, Y. Computation-Accelerated Design of Materials and Interfaces for All-Solid-State Lithium-Ion Batteries. *Joule* **2018**, *2*, 2016−2046.

(105) Ahmad, Z.; Xie, T.; Maheshwari, C.; Grossman, J. C.; Viswanathan, V. Machine Learning Enabled Computational Screening of Inorganic Solid Electrolytes for Suppression of Dendrite Formation in Lithium Metal Anodes. *ACS Cent. Sci.* **2018**, *4*, 996−1006.

(106) Huo, H.; Chen, Y.; Luo, J.; Yang, X.; Guo, X.; Sun, X. Rational Design of Hierarchical "Ceramic-in-Polymer" and "Polymer-in-Ceramic" Electrolytes for Dendrite-Free Solid-State. *Adv. Energy Mater.* **2019**, *9*, 1804004.